

Astrocytic abnormalities and global DNA methylation patterns in depression and suicide

Corina Nagy, B.Sc.^{1,2}, Matthew Suderman, Ph.D.^{4,5}, Jennie Yang, M.Sc.¹, Moshe Szyf, Ph.D.^{5,6}, Naguib Mechawar, Ph.D.^{1,2,3}, Carl Ernst, Ph.D.^{1,3}, and Gustavo Turecki, M.D., Ph.D.^{1,2,3}

¹McGill Group for Suicide Studies, Douglas Mental Health University Institute

²Integrated Program in Neuroscience

³Department of Psychiatry

⁴McGill Centre for Bioinformatics

⁵Sackler Program for Epigenetics & Developmental Psychobiology

⁶Department of Pharmacology and Therapeutics

Abstract

Astrocytes are glial cells specific the central nervous system involved in numerous brain functions including regulation of synaptic transmission and of immune reactions. There is mounting evidence suggesting astrocytic dysfunction in psychopathologies such as major depression, however, little is known about the underlying etiological mechanisms. Here we report a two-stage study investigating genome-wide DNA methylation associated with astrocytic markers in depressive psychopathology. We first characterized prefrontal cortex samples from 121 individuals (76 who died during a depressive episode and 45 healthy controls) for the astrocytic markers *GFAP*, *ALDH1L1*, *SOX9*, *GLUL*, *SCL1A3*, *GJA1*, and *GJB6*. A subset of 22 cases with consistently downregulated astrocytic markers was then compared to 17 matched controls using MBD2-sequencing followed by validation with high resolution melting and bisulfite Sanger sequencing. With these data, we generated a genome-wide methylation map unique to altered astrocyte-associated depressive psychopathology. The map revealed differentially methylated regions (DMRs) between cases and controls, the majority of which displayed reduced methylation levels in cases. Among intragenic DMRs, *GRIK2* and *BEGAIN* were the most significant, and also significantly correlated with genes expression. Cell sorted fractions were investigated and demonstrated an important non-neuronal contribution of methylation status in *BEGAIN*. Functional cell assays revealed promoter and enhancer-like properties in this region, which were markedly decreased by methylation. Furthermore, a large number of our DMRs overlapped known ENCODE identified regulatory elements. Taken together, our data indicate significant differences in the methylation patterns specific to astrocytic dysfunction associated with depressive psychopathology, providing a potential framework for better understanding this disease phenotype.

Keywords

Astrocytes; mental Health; DNA methylation; epigenomics; genetics; depression

Introduction

Glial cells account for at least 75% of brain cells ¹, and are implicated in a range of psychiatric disorders, including alcoholism ², schizophrenia ³, depression⁴ and suicide ^{5, 6}. In particular, astrocytic dysfunction is evident in depressive psychopathologies, including suicide⁴. Astrocytes are multifaceted cells with numerous functions, including regulation of blood flow, synaptic communication and plasticity, immune regulation ⁷ and maintenance of neuronal functioning⁸. These - and other - physiological roles are likely impacted in depression and suicide given evidence from postmortem and animal studies showing altered astrocytic morphologies ⁵ and persistently decreased expression of astrocyte-specific genes, such as glial fibrillary acidic protein (GFAP) ⁹, glutamine synthetase (GLUL)¹⁰, the glial high affinity transporters, SLC1A2 and SLC1A3 ¹⁰, aquaporin 4 (AQP4) ¹¹ and the connexin genes Cx30 and Cx43 ⁶.

Despite consistent reports, little is known about the underlying etiological mechanisms linking astrocytic dysfunction to depression and suicide. These could involve epigenetic factors such as DNA methylation, which stably modulates gene expression. Indeed, DNA methylation changes at specific genomic loci are associated with increased risk of psychopathology ^{12, 13}. The purpose of the current study was to identify DNA methylation patterns associated with astrocytic alterations in depression and suicide. To this end, we characterized expression of astrocytic markers *GFAP*, *ALDH1L1*, *SLC1A3*, *GJA1*, *GJB6*, *GLUL* and *SOX9* in the dorsolateral prefrontal cortex of individuals having died by suicide and sudden death controls. For all subjects with consistent and pronounced down-regulation of astrocytic markers, we conducted methylation binding domain (MBD) enrichment coupled with next-generation sequencing. Our results suggest a framework to better understand how astrocyte dysfunction impacts depression and suicide.

Materials and Methods

Brain samples, clinical characterization and group composition

Brain tissue was obtained from the Douglas-Bell Canada Brain Bank (DBCBB; <http://www.douglas.qc.ca/page/brain-bank>). The DBCBB recruits suicide cases and sudden death control subjects. To avoid prolonged agonal states, both cases and controls recruited to the bank cannot undergo resuscitation procedures or medical intervention. Brain tissue for the DBCBB is collected after consent is obtained from next-of-kin. Families are recontacted after approximately 4 months to undergo a series of structured interviews, known as psychological autopsies, with the person best acquainted with the deceased, as described elsewhere ¹⁴. Interviews are supplemented with information from archival material obtained from hospitals, the Coroner's office or social services. Following the interviews, clinical vignettes are produced and assessed by a panel of clinicians to generate DSM-IV diagnoses.

This is a well-accepted and valid procedure to obtain clinical information on deceased individuals through proxy-based interviews^{15, 16}.

Cases in this study were individuals who died by suicide as determined by the Coroner, and following psychological autopsies met criteria for major depressive disorder or had no axis I, but with evidence of depressive symptoms at the moment of death. Controls were individuals who died suddenly in motor vehicle accidents or by cardiac arrest, and did not have evidence of axis I disorders. For preliminary screening, we included 121 brain samples (76 cases) and tested two cortical brain regions. Low expressors were identified using tissue from Brodmann area (BA) 10 then replicated in tissue from BA 8/9. Only tissue from the left hemisphere (grey matter only) was used. These cortical regions are consistently implicated in depression^{17–20} and are involved in higher order functioning such as decision-making, that is impaired in suicide²¹.

The second part of this study used expression profiles to define the case group. Specifically, at least 5 of the 7 genes investigated had to be in the lowest quartile (n=22) of expression (SI Figure 1–3). Controls were selected based on age, gender and PMI to group match the suicide group; gene expression was not used to select controls. The average PMI (\pm S.E.M) for controls was 18.8 (\pm 2.91) and cases 17.7 (\pm 4.48). The average age of controls was 41.3 (\pm 5.87) and suicides 41.0 (\pm 2.64) and the average RIN for controls was 6.2 (\pm 0.16) and suicide 6.4 (\pm 0.16). There was no significant difference between groups for any of these variables. This study was approved by the Douglas Institute Research Ethics Board.

Methods for histological sectioning, gene expression analysis, methylation binding domain protein sequencing (MBD-Seq), sequencing analysis, ENCODE analysis, high resolution melting and site-specific bisulfite sequencing, fluorescence assisted cell sorting (FACs), and functional cell assays can be found in the online supplemental information (SI Methods).

Results

Identification of cases with low expression of astrocyte-related genes

To identify subjects with potential astrocytic dysfunction, we screened prefrontal cortical (PFC) samples obtained from the DBCBB for expression levels of genes exclusively or primarily expressed in astrocytes. This initial screen was conducted on 121 subjects (87 males), including 76 individuals who died by suicide, and 45 sudden death controls. We selected the following 7 genes for screening based on their high expression in astrocytes: *GFAP*, *ALDH1L1*, *SOX9*, *GLUL*, *SCL1A3*, *GJA1*, and *GJB6*, all showing significantly decreased expression in cases compared to controls (Figure 1). To demonstrate that these results specifically reflected a decrease in astrocyte gene expression, we examined the level of NeuN (aka *RBFOX3*), a well-known marker of neurons²² and found no significant difference between cases and controls (Figure 1h).

Epigenetic factors are known to regulate gene expression and may contribute to the astrocytic dysfunction observed in our cases. Specifically, we hypothesized that DNA methylation patterns differ between groups. To test this, we conducted a genome-wide methylation sequencing study focusing on individuals with the most severe molecular

phenotype. We selected cases showing the lowest mRNA expression levels of the astrocyte marker genes used for screening, and operationally defined extreme cases by expression levels in the bottom quartile for at least 5 of the 7 genes; 22 cases met these criteria (SI Figures 1–5, SI Tables 1–2). Cases were compared with 17 psychiatrically normal controls grouped-matched according to age, RIN, post-mortem interval and gender. To decrease variability, all subjects included in the analysis were males.

Generation of high quality genome-wide MBD2-seq profiles

We performed genome-wide DNA methylation analysis by isolating fragmented DNA using biotinylated-MBD2. The MBD2 protein specifically targets densely methylated CpGs²³ and does not target hydroxymethylated cytosines^{23,24} thus sequencing MBD2-enriched DNA identifies methylated regions from the whole genome. Comparing the number of sequenced reads matching each region enabled us to identify methylation differences between cases and controls. Many quality control steps were performed to insure high quality (SI Figures 6–7 SI Table 3)

In total, we obtained nearly 450 million reads, and mean read counts were similar between groups (Student T test, $p=0.85$) (SI Table 4). Our reads provided 20x coverage per base for the MBD enrichment (SI Figure 8). We assessed our data for genomic metrics, irrespective of disease status. First, we assessed the consistency of sequencing data by measuring overall methylation levels at specific genomic features. DNA methylation levels were consistent with expectations at all genomic loci assessed: CpG islands showed the least amount of methylation, first exons showed less methylation than other exons and imprinted regions showed increased levels of methylation (Figure 2a, Wilcoxin rank-sum, $p < 2E10-22$).

Second, to validate the enrichment of methylated reads and to confirm bioinformatic processing, we selected regions of the genome identified in sequencing data as either highly methylated or poorly methylated and re-performed MBD2 enrichment reactions using identical DNA samples as the initial sequencing reaction. We found that levels identified as highly methylated in the sequencing reaction gave the lowest Ct values in qRT-PCR analysis, and the opposite was found in genomic regions with low methylation (region 1: $r=-0.81$, $t=0.025$; region 2 $r=-0.74$, $t=0.047$; region 3: $r=-0.61$, $t=0.09$) (SI Figure 9).

Differentially methylated regions in cases and controls

After ensuring quality and accuracy of MBD2 enrichment, we assessed case and control group differences. There were 115 differentially methylated regions (DMRs) across the genome. Of these, 33.91% ($N = 34$) were found in genes, almost all intragenic and falling within introns ($N= 31$; 31.3%). Nearly 11% ($N=14$) of DMRs were within promoters, defined as sequences up to 5Kb upstream of transcription start sites (Figure 2b). However, the majority of DMRs were found in intergenic regions 56.6% ($N=66$).

As expected, the number of reads mapping back to each chromosome strongly correlated with their size (spearman $r=0.83$, $p < 0.0001$), while there was no difference in the contribution of each group to chromosome coverage (SI Figure 10a,b). We found no relationship between chromosome size and location of DMR, i.e., DMRs were independent of size and read count (Spearman $r=-0.15$, $p=0.48$) (SI Figure 10c).

Most DMRs were hypomethylated in cases. There was considerable decrease in methylation within the gene body of cases; 58.8% of the within gene DMRs were less methylated in cases compared to controls, and these results were consistent in the intergenic regions, where a similar percentage of DMRs were hypomethylated (57.6%) (Figure 2c).

We observed two genomic regions enriched with DMRs clusters: one on chromosome 10 and another on the X chromosome (Fisher's exact test, FDR < 0.05; SI Table 5 and SI Figure 11). The DMRs in these two regions overlapped strongly with ENCODE elements suggesting potentially important regulatory roles²⁵.

Functional relevance of DMRs derived from ENCODE data

Using publically available data from the Encyclopedia of DNA elements (ENCODE), we performed an in-silico assessment of the regulatory potential of each DMR by identifying overlaps with ENCODE features. Altogether, we assessed 41 ENCODE features which include histone modifications and DNA binding proteins known to influence gene transcription. Our analysis showed enrichment for 37 of the 41 features in hypomethylated regions (Fisher's exact test average $p < 4.82E-03$, SI Table 6); however, there was no enrichment in hypermethylated sites. Nearly half the DMRs contained at least one ENCODE feature (Figure 3a). Histone 3 lysine 4 trimethylation (H3K4me3), a chromatin modification enriched in gene promoters and most often associated with euchromatin and active transcription²⁶, and DNase I hypersensitivity sites (DHSs) which are associated with many *cis*-regulatory elements including promoters, enhancers, insulators, silencers and locus control regions²⁷, overlapped most frequently with the DMRs (Figure 3b). Both features overlapped with 22.6% of DMRs. As DHSs have been shown to precede promoter regions marked by H3K4me3²⁷, it was not surprising that most DHS sites overlapped with H3K4me3. We found 4 DMRs with an impressive overlap of 20 or more ENCODE features. These regions were found in the pericentromeric region of 4 different chromosomes (4,7,16 and 21). One of the most conserved functions of DNA methylation is stabilizing pericentromeric repeats by inhibiting their latent transcriptional potential²⁸. Moreover, decondensing of these heterochromatic regions can result in illegitimate rearrangements²⁹, therefore hypomethylation in these regions often lead to notable consequences.

To assess the permissive or inhibitory relationship of the ENCODE data with our data, we grouped the ENCODE features into active or repressive marks based on their known function (SI Tables 6–8). The distribution of DMRs falling into each category was comparable, with 45% overlapping repressive elements and 55% overlapping active elements.

Differentially methylated astrocytic genes

As our subjects were selected based on astrocytic expression patterns, we were interested in potential associations between DMRs and astrocyte and/or astrocyte-regulatory genes. To assess whether these genes were associated with DMRs, we conducted gene ontology analyses focusing on genes highly expressed in astrocytes and genes coding for regulatory factors of astrocytic expression. There were 4 astrocyte-associated genes coded within

regions of differential methylation (Table 1), containing multiple sites of differential methylation. These represented 21% of the gene-associated DMRs.

Gene specific validation of DMRs showed inverse correlation to gene expression levels

We validated the most significant DMRs, focusing on the DMRs related to astrocytic function (Table 1) and the complete intragenic DMRs (SI Table 10). These DMRs were, respectively, in *GRIK2* and *BEGAIN* (Figure 4a–b). *GRIK2* is implicated in astrocytic function and has been associated with mood disorders^{30–33}, whereas *BEGAIN* is associated with cellular communication³⁴. For validation, we performed both bisulfite cloning (Bs-Cloning) and High Resolution Melting analysis (HRM). In both cases, DMRs were consistent with the MBD-seq analysis, though as expected, HRM showed less sensitivity. HRM results are presented in figure 4c and 4g, and show significant differences for both *GRIK2* (Student T-test, $p=0.02$) and *BEGAIN* (Student t-test, $p=0.007$) in the same direction observed with the MBD-Seq data. With Bs-cloning, we achieved base-pair resolution of methylation levels for *GRIK2* and *BEGAIN*, which strongly supported the MBD-Seq data. (Figures 4d, h and SI Table 9a and b). Next, we measured expression levels for each gene, finding an increase in *GRIK2* expression in cases (Figure 4f, $p=0.012$). For *BEGAIN*, there are two major transcripts with little known about their expression patterns. We investigated brain and peripheral tissues, and found that variant 1 has increased expression in the brain (Figure 4j). When we assessed expression of *BEGAIN* transcripts, we observed a marked decrease of variant 1 in cases (2.3 fold decrease, $p<0.0001$), while variant 2 remained unchanged (Figure 4k–l). Analysis of cluster CpGs methylation and expression showed a significant inverse correlation for both *GRIK2* (Figure g, $r=-0.37$, $p<0.05$) and *BEGAIN* (Figure 4n, $r=-0.37$, $p<0.05$), suggesting a role for methylation regulating expression in these genes.

Non-Neuronal cells from case samples drive methylation difference in *BEGAIN*

As DNA methylation is known to be cell-type specific, we used fluorescence assisted cell sorting to separate tissue homogenates into neuronal and non-neuronal fractions. While it is currently methodologically challenging to isolate astrocytic fractions from frozen tissue, the non-neuronal fraction is primarily composed of astrocytes as they make up the bulk of non-neuronal cells of the human brain. We collected nuclei marked with NeuN and unmarked nuclei for all samples. DNA from each fraction was directly bisulfite converted, then subjected to cloning and Sanger sequencing as for validation of brain homogenates. For *GRIK2*, we observed no difference in methylation across cell types (SI Figure 14d), however, for *BEGAIN* we observed a marked increase of methylation for cases in the non-neuronal fraction, suggesting that the sizeable difference in methylation between cases and controls was largely driven by non-neuronal cells (Figure 4j, one-way anova, $F(3, 32) = 10.74$, $P < 0.0001$).

DNA methylation in DMR represses transcription

Considering the strong increase of methylation detected in both the homogenate and non-neuronal cellular fraction of *BEGAIN*, we decided to assess this region in a functional cell assay to determine the direct consequences of methylation. As suggested by the CHROMHMM from ENCODE (SI Figure 15), this region of *BEGAIN* has both promoter

and enhancer capabilities, therefore the 474bp amplicon was inserted into 2 separate CpG-free vectors, one containing no endogenous promoter (Figure 5a) to test potential promoter activity and a second under the control of the human EF-1 α promoter to test enhancer-like activity (Figure 5b). The inserted amplicons were either fully methylated or fully unmethylated, the report assays were performed in quintuplicate and repeated twice independently. This 474bp region of *BEGAIN* clearly showed promoter activity, which was fully repressed by methylation (Figure 5c Kruskal Wallis =19.94, d.f, 3, $p<0.0001$, SI Figure 15a–b). Equally, when this region of *BEGAIN* was inserted in an enhancer position next to the human EF-1 α promoter, methylation caused complete loss of reporter gene expression (Figure 5d, Kruskal Wallis= 22.15, d.f, 3, $p<0.0001$, SI Figure 15c–d). These results indicate a potent effect of DNA methylation on this region of *BEGAIN* and suggest a potentially causative role of methylation in the downregulation of the *BEGAIN* variant 1 we observed in cases with astrocytic dysfunction.

Discussion

In this study, we investigated genomic DNA methylation patterns that may contribute to astrocyte dysfunction in depression and suicide. First, we characterized groups for their expression profile of several astrocyte-associated genes in the prefrontal cortex. Subsequently, we conducted MBD-Seq focusing on cases with clear astrocytic dysfunction at a molecular level. The profiles generated in our study revealed differential DNA methylation at multiple loci, including ENCODE associated regulatory sequences. In following-up our top intragenic DMRs we were able to replicate our findings using two independent techniques, and in addition, we found that the methylation differences correlated with gene expression changes. Furthermore we demonstrated that in cases, non-neuronal cells drive methylation changes observed in *BEGAIN*. Lastly, we showed through functional cell assays that methylation of our isolated region in *BEGAIN* almost completely abolishes reporter gene expression in vitro. This is, to our knowledge, the first study using next-generation sequencing to investigate genome-wide differential methylation associated with depression and suicide.

Most DNA methylation studies use candidate approaches; among the strengths of the current study is the genome-wide approach coupled by DNA sequencing. Studies in rats and humans have shown discrete regions of hypermethylation associated with behavioural phenotypes and transcriptional regulation^{35, 36}. These studies used candidate gene approaches or were focused on promoter sequences³⁷. In the present study, we avoided restricting our analyses to promoter regions, and provided an unbiased view of DNA methylation associated with depressive psychopathology and suicide. About 90% of the DMRs were found in non-promoter regions where the relationship with expression is variable. We found many DMRs in gene bodies, where methylation is commonly associated with active transcription³⁸. Our results are consistent with a regulatory mechanism for repressing transcription in these regions. For example, a reduction of gene body methylation can result in *de novo* histone modifications³⁹ that decrease transcription. As many of the DMRs in this study were found within gene bodies and intergenically, hypomethylation may result in gene repression.

Our study provides valuable information about often-overlooked regions of the genome⁴⁰. In support of our findings, most variability in methylation occurs in gene bodies and intergenic regions, rather than promoters and upstream regulatory regions⁴¹. We identified two cluster regions, on chromosome 10 and the X chromosome, where DMRs fell primarily on short (SINEs) and long interspersed element (LINEs). DNA methylation maintains the stability of the genome by silencing these mobile elements⁴². Decreased methylation and increased expression of these elements could disrupt gene transcription. In addition, reduced methylation in these clusters could alter associated chromatin⁴³. Moreover, four of the DMRs that we found within pericentromeric regions overlapped with over 20 ENCODE elements, representing regions under extensive epigenetic control. Abnormal methylation in these regions is implicated in developmental disorders⁴⁴ suggesting important functional consequences⁴⁵

Among intragenic DMRs, we selected two according to significance for additional work: *GRIK2* and *BEGAIN*. *GRIK2* codes for glutamate ionotropic kainate receptor, which is a ligand-gated cation channel. This channel is associated with grey and white matter astrocytes³⁰, and altered calcium signaling in response to antidepressants³². *GRIK2* has been previously associated with psychiatric or neurological disorders^{30–32, 49}, including with depression^{30–32}. Our combined data showed that *GRIK2* is hypomethylated in intron 13 in cases as compared to controls, and we suspect that this intronic region of hypomethylation may influence alternative splicing of *GRIK2*⁵⁰, potentially favoring the protein isoform with reduced permeability calcium signaling, however additional work is required to explore this hypothesis.

BEGAIN (brain-enriched guanylate kinase-associated protein), on the other hand, showed on average a 3-fold increase in methylation in cases, representing one of the strongest changes reported to date in psychiatric phenotypes. *BEGAIN*, is poorly studied in humans, but has been associated with diabetes and autoimmune disorders⁵¹ an interesting finding considering the growing evidence for the inflammatory basis of depression^{52, 53} and the role of astrocytes in the regulation of neuroinflammation⁵⁴. In addition, a study in rats has shown increased *BEGAIN* expression in the frontal pole in response to prenatal stress as a paradigm for the etiology of schizophrenia.⁵⁵ *BEGAIN* is highly associated to the postsynaptic density proteins, and particularly to the postsynaptic density 95 (PSD95)^{34, 56, 57}, having 90% co-localization with PSD95⁵⁶, and a role in sustaining the structure of this scaffolding protein⁵⁸. PSD95 is the protein found in the postsynaptic dendritic heads of excitatory synapses, and has been implicated in the coordination of the downstream communication of glutamate receptors, including *GRIK2*, through the binding of PSD95 to its guanylate kinase domains⁵⁹. Recently, it has been shown that the astrocytes forming part of this excitatory synapse may play an important role in regulating the excitatory/inhibitory balance of neurons through PSD95⁶⁰. The epigenetic alterations to *BEGAIN* and *GRIK2* and their association to astrocytically mediated PSD95, suggests possible defective synaptic communication and/or synaptic plasticity⁵⁷.

Interestingly, our two top hits are involved in synaptic communication and regulation^{34, 61}. Whereas *GRIK2* is known to be expressed in astrocytes and to be directly involved in astrocyte-mediated responses to antidepressant drugs^{31, 32, 49}, *BEGAIN* has no known

association to astrocytes. However, as the primary contribution of methylation was found in non-neuronal cells, it appears that astrocytes have a functional role in the regulation of this gene via methylation alterations. Otherwise, this would not be the first time that changes to genes in astrocytes at an epigenetic level are seen to influence normal neuronal function. For instance, Tao and colleagues showed that selectively knocking-out Dicer in astrocytes leads to neuronal dysfunction and degeneration⁶². Thus far *BEGAIN* has been investigated and localized in nuclei and synapses of neurons⁵⁶, but there is no information on its relation to astrocytes. Much like *GRIK2*, *BEGAIN* could play an important role in both cell types. Since *BEGAIN* is thought to maintain the structure of the post-synaptic density it would be interesting to see if the strong reduction of its transcript results in altered dendritic morphology as has become one of the emerging theories of autism, schizophrenia and Alzheimer's⁶³. This study has opened the door to this and many other questions.

Our study is not without limitations. MBD2 has a higher affinity to densely methylated CpGs than antibody-based approaches; therefore we may be missing single base pair differences. Conversely, MBD is able to discriminate between 5' hydroxymethylcytosine and 5' methylcytosine²⁴ with greater efficiency than the monoclonal antibody directed against 5-methylcytosine⁶⁴. Regarding our sample selection, altered transcription is often used as a marker for astrocytic dysfunction^{6, 9, 10}, however, astrocyte dysfunction can be defined in many ways and may not be reflected by gene expression differences. Finally we limited this study to DNA methylation changes and thus did not examine other epigenetic mechanism that may be involved in gene regulation. Despite these limitations, our study produced a list of differentially methylated regions showing clear evidence of astrocytic dysfunction in individuals who were depressed and died by suicide. Furthermore we identified two genes involved in synaptic communication, *GRIK2* and *BEGAIN*, which appear to be regulated by DNA methylation in cases with astrocytic dysfunction. Each DMR identified here provides avenues for further investigation of the pathophysiological mechanisms underlying astrocytic dysfunction in mood disorders.

Supplementary Material

Refer to Web version on PubMed Central for supplementary material.

Acknowledgments

We thank the members of the next generation sequencing platform at Genome Quebec, and acknowledge the expert help of the DBCBB staff. C.N is supported by a scholarship from the FRQS. CE is supported by the Canada Research Chairs program. NM is a CIHR New Investigator and Bell Senior Fellow in Mental Health. GT is a national researcher from FRQS. This study was funded by a CIHR operating grant (MOP# 119429).

References

1. Kettenmann, H., Ransom, BR. Neuroglia. 2. Oxford University Press; New York: 2005. p. xixp. 601
2. Hercher C, Parent M, Flores C, Canetti L, Turecki G, Mechawar N. Alcohol dependence-related increase of glial cell density in the anterior cingulate cortex of suicide completers. Journal of psychiatry & neuroscience: JPN. 2009; 34(4):281–288. [PubMed: 19568479]
3. Bernstein H-G, Steiner J, Bogerts B. Glial cells in schizophrenia: pathophysiological significance and possible consequences for therapy. Expert review of neurotherapeutics. 2009; 9(7):1059–1071. [PubMed: 19589054]

4. Rajkowska G, Stockmeier CA. Astrocyte pathology in major depressive disorder: insights from human postmortem brain tissue. *Curr Drug Targets*. 2013
5. Torres-Platas S, Hercher C, Davoli M, Maussion G, Labonté B, Turecki G, et al. Astrocytic hypertrophy in anterior cingulate white matter of depressed suicides. *Neuropsychopharmacology: official publication of the American College of Neuropsychopharmacology*. 2011; 36(13):2650–2658. [PubMed: 21814185]
6. Ernst C, Nagy C, Kim S, Yang J, Deng X, Hellstrom I, et al. Dysfunction of astrocyte connexins 30 and 43 in dorsal lateral prefrontal cortex of suicide completers. *Biological psychiatry*. 2011; 70(4): 312–319. [PubMed: 21571253]
7. Oberheim N, Goldman S, Nedergaard M. Heterogeneity of astrocytic form and function. *Methods in molecular biology (Clifton, NJ)*. 2012:814.
8. Sidoryk-Wegrzynowicz M, Wegrzynowicz M, Lee E, Bowman AB, Aschner M. Role of astrocytes in brain function and disease. *Toxicologic pathology*. 2011; 39(1):115–123. [PubMed: 21075920]
9. Si X, Miguel-Hidalgo J, O'Dwyer G, Stockmeier C, Rajkowska G. Age-dependent reductions in the level of glial fibrillary acidic protein in the prefrontal cortex in major depression. *Neuropsychopharmacology: official publication of the American College of Neuropsychopharmacology*. 2004; 29(11):2088–2096. [PubMed: 15238995]
10. Choudary P, Molnar M, Evans S, Tomita H, Li J, Vawter M, et al. Altered cortical glutamatergic and GABAergic signal transmission with glial involvement in depression. *Proceedings of the National Academy of Sciences of the United States of America*. 2005; 102(43):15653–15658. [PubMed: 16230605]
11. Bernard R, Kerman IA, Thompson RC, Jones EG, Bunney WE, Barchas JD, et al. Altered expression of glutamate signaling, growth factor, and glia genes in the locus coeruleus of patients with major depression. *Mol Psychiatry*. 2011; 16(6):634–646. [PubMed: 20386568]
12. Turecki G, Ernst C, Jollant F, Labonte B, Mechawar N. The neurodevelopmental origins of suicidal behavior. *Trends Neurosci*. 2012; 35(1):14–23. [PubMed: 22177979]
13. Nagy C, Turecki G. Sensitive periods in epigenetics: bringing us closer to complex behavioral phenotypes. *Epigenomics*. 2012; 4(4):445–457. [PubMed: 22920183]
14. Dumais A, Lesage AD, Alda M, Rouleau G, Dumont M, Chawky N, et al. Risk factors for suicide completion in major depression: a case-control study of impulsive and aggressive behaviors in men. *Am J Psychiatry*. 2005; 162(11):2116–2124. [PubMed: 16263852]
15. Arsenault-Lapierre G, Kim C, Turecki G. Psychiatric diagnoses in 3275 suicides: a meta-analysis. *BMC Psychiatry*. 2004; 4:37. [PubMed: 15527502]
16. Isometsa ET. Psychological autopsy studies--a review. *Eur Psychiatry*. 2001; 16(7):379–385. [PubMed: 11728849]
17. Sequeira A, Morgan L, Walsh DM, Cartagena PM, Choudary P, Li J, et al. Gene expression changes in the prefrontal cortex, anterior cingulate cortex and nucleus accumbens of mood disorders subjects that committed suicide. *PloS one*. 2012; 7(4):e35367. [PubMed: 22558144]
18. Kang H, Voleti B, Hajszan T, Rajkowska G, Stockmeier C, Licznarski P, et al. Decreased expression of synapse-related genes and loss of synapses in major depressive disorder. *Nature medicine*. 2012; 18(9):1413–1417.
19. Goswami D, Jernigan C, Chandran A, Iyo A, May W, Austin M, et al. Gene expression analysis of novel genes in the prefrontal cortex of major depressive disorder subjects. *Progress in neuro-psychopharmacology & biological psychiatry*. 2012; 43C:126–133.
20. Underwood M, Kassir S, Bakalian M, Galfalvy H, Mann J, Arango V. Neuron density and serotonin receptor binding in prefrontal cortex in suicide. *The international journal of neuropsychopharmacology/official scientific journal of the Collegium Internationale Neuropsychopharmacologicum (CINP)*. 2012; 15(4):435–447.
21. Kim S, Lee D. Prefrontal cortex and impulsive decision making. *Biol Psychiatry*. 2011; 69(12): 1140–1146. [PubMed: 20728878]
22. Dent M, Segura-Anaya E, Alva-Medina J, Aranda-Anzaldo A. NeuN/Fox-3 is an intrinsic component of the neuronal nuclear matrix. *FEBS letters*. 2010; 584(13):2767–2771. [PubMed: 20452351]

23. Li N, Ye M, Li Y, Yan Z, Butcher L, Sun J, et al. Whole genome DNA methylation analysis based on high throughput sequencing technology. *Methods (San Diego, Calif)*. 2010; 52(3):203–212.
24. Mellén M, Ayata P, Dewell S, Kriaucionis S, Heintz N. MeCP2 Binds to 5hmC Enriched within Active Genes and Accessible Chromatin in the Nervous System. *Cell*. 2012; 151(7):1417–1430. [PubMed: 23260135]
25. Tomilin N. Regulation of mammalian gene expression by retroelements and non-coding tandem repeats. *BioEssays: news and reviews in molecular, cellular and developmental biology*. 2008; 30(4):338–348.
26. Koch C, Andrews R, Flicek P, Dillon S, Karaöz U, Clelland G, et al. The landscape of histone modifications across 1% of the human genome in five human cell lines. *Genome research*. 2007; 17(6):691–707. [PubMed: 17567990]
27. Thurman RE, Rynes E, Humbert R, Vierstra J, Maurano MT, Haugen E, et al. The accessible chromatin landscape of the human genome. *Nature*. 2012; 489(7414):75–82. [PubMed: 22955617]
28. Lehnertz B, Ueda Y, Derijck AA, Braunschweig U, Perez-Burgos L, Kubicek S, et al. Suv39h-mediated histone H3 lysine 9 methylation directs DNA methylation to major satellite repeats at pericentric heterochromatin. *Curr Biol*. 2003; 13(14):1192–1200. [PubMed: 12867029]
29. DeJardin J. How chromatin prevents genomic rearrangements: locus colocalization induced by transcription factor binding. *Bioessays*. 2012; 34(2):90–93. [PubMed: 22086436]
30. Brand-Schieber E, Werner P. AMPA/kainate receptors in mouse spinal cord cell-specific display of receptor subunits by oligodendrocytes and astrocytes and at the nodes of Ranvier. *Glia*. 2003; 42(1):12–24. [PubMed: 12594733]
31. Li B, Zhang S, Li M, Zhang H, Hertz L, Peng L. Down-regulation of GluK2 kainate receptor expression by chronic treatment with mood-stabilizing anti convulsants or lithium in cultured astrocytes and brain, but not in neurons. *Neuropharmacology*. 2009; 57(4):375–385. [PubMed: 19596362]
32. Li B, Zhang S, Zhang H, Hertz L, Peng L. Fluoxetine affects GluK2 editing, glutamate-evoked Ca(2+) influx and extracellular signal-regulated kinase phosphorylation in mouse astrocytes. *Journal of psychiatry & neuroscience: JPN*. 2011; 36(5):322–338. [PubMed: 21320410]
33. Li H, Durbin R. Fast and accurate long-read alignment with Burrows-Wheeler transform. *Bioinformatics (Oxford, England)*. 2010; 26(5):589–595.
34. Deguchi M, Hata Y, Takeuchi M, Ide N, Hirao K, Yao I, et al. BEGAIN (brain-enriched guanylate kinase-associated protein), a novel neuronal PSD-95/SAP90-binding protein. *The Journal of biological chemistry*. 1998; 273(41):26269–26272. [PubMed: 9756850]
35. Weaver IC, Diorio J, Seckl JR, Szyf M, Meaney MJ. Early environmental regulation of hippocampal glucocorticoid receptor gene expression: characterization of intracellular mediators and potential genomic target sites. *Ann N Y Acad Sci*. 2004; 1024:182–212. [PubMed: 15265782]
36. Labonte B, Yerko V, Gross J, Mechawar N, Meaney MJ, Szyf M, et al. Differential glucocorticoid receptor exon 1(B), 1(C), and 1(H) expression and methylation in suicide completers with a history of childhood abuse. *Biol Psychiatry*. 2012; 72(1):41–48. [PubMed: 22444201]
37. Labonte B, Suderman M, Maussion G, Navaro L, Yerko V, Mahar I, et al. Genome-wide epigenetic regulation by early-life trauma. *Arch Gen Psychiatry*. 2012; 69(7):722–731. [PubMed: 22752237]
38. Meissner A, Mikkelsen T, Gu H, Wernig M, Hanna J, Sivachenko A, et al. Genome-scale DNA methylation maps of pluripotent and differentiated cells. *Nature*. 2008; 454(7205):766–770. [PubMed: 18600261]
39. Hahn MA, Wu X, Li AX, Hahn T, Pfeifer GP. Relationship between gene body DNA methylation and intragenic H3K9me3 and H3K36me3 chromatin marks. *PloS one*. 2011; 6(4):e18844. [PubMed: 21526191]
40. Gerstein M, Kundaje A, Hariharan M, Landt S, Yan K-K, Cheng C, et al. Architecture of the human regulatory network derived from ENCODE data. *Nature*. 2012; 489(7414):91–100. [PubMed: 22955619]
41. Consortium EP, Dunham I, Kundaje A, Aldred S, Collins P, Davis C, et al. An integrated encyclopedia of DNA elements in the human genome. *Nature*. 2012; 489(7414):57–74. [PubMed: 22955616]

42. Carnell AN, Goodman JI. The long (LINEs) and the short (SINEs) of it: altered methylation as a precursor to toxicity. *Toxicological sciences: an official journal of the Society of Toxicology*. 2003; 75(2):229–235. [PubMed: 12773759]
43. Chueh AC, Northrop EL, Brettingham-Moore KH, Choo KH, Wong LH. LINE retrotransposon RNA is an essential structural and functional epigenetic component of a core neocentromeric chromatin. *PLoS Genet*. 2009; 5(1):e1000354. [PubMed: 19180186]
44. Xu GL, Bestor TH, Bourc'his D, Hsieh CL, Tommerup N, Bugge M, et al. Chromosome instability and immunodeficiency syndrome caused by mutations in a DNA methyltransferase gene. *Nature*. 1999; 402(6758):187–191. [PubMed: 10647011]
45. Smith ZD, Meissner A. DNA methylation: roles in mammalian development. *Nat Rev Genet*. 2013; 14(3):204–220. [PubMed: 23400093]
46. Sundaram SK, Huq AM, Sun Z, Yu W, Bennett L, Wilson BJ, et al. Exome sequencing of a pedigree with Tourette syndrome or chronic tic disorder. *Annals of neurology*. 2011; 69(5):901–904. [PubMed: 21520241]
47. Scharf JM, Miller LL, Mathews CA, Ben-Shlomo Y. Prevalence of Tourette syndrome and chronic tics in the population-based Avon longitudinal study of parents and children cohort. *Journal of the American Academy of Child and Adolescent Psychiatry*. 2012; 51(2):192–201. e195. [PubMed: 22265365]
48. Grupe A, Li Y, Rowland C, Nowotny P, Hinrichs A, Smemo S, et al. A scan of chromosome 10 identifies a novel locus showing strong association with late-onset Alzheimer disease. *American journal of human genetics*. 2006; 78(1):78–88. [PubMed: 16385451]
49. Li B, Dong L, Fu H, Wang B, Hertz L, Peng L. Effects of chronic treatment with fluoxetine on receptor-stimulated increase of [Ca²⁺]_i in astrocytes mimic those of acute inhibition of TRPC1 channel activity. *Cell calcium*. 2011; 50(1):42–53. [PubMed: 21640379]
50. Wan J, Oliver VF, Zhu H, Zack DJ, Qian J, Merbs SL. Integrative analysis of tissue-specific methylation and alternative splicing identifies conserved transcription factor binding motifs. *Nucleic Acids Res*. 2013; 41(18):8503–8514. [PubMed: 23887936]
51. Wallace C, Smyth D, Maisuria-Armer M, Walker N, Todd J, Clayton D. The imprinted DLK1-MEG3 gene region on chromosome 14q32. 2 alters susceptibility to type 1 diabetes. *Nature Genetics*. 2010; 42(1):68–71. [PubMed: 19966805]
52. Miller AH, Maletic V, Raison CL. Inflammation and its discontents: the role of cytokines in the pathophysiology of major depression. *Biol Psychiatry*. 2009; 65(9):732–741. [PubMed: 19150053]
53. Raedler TJ. Inflammatory mechanisms in major depressive disorder. *Current opinion in psychiatry*. 2011; 24(6):519–525. [PubMed: 21897249]
54. Jasna, Kritz. Neuron-Astrocyte Interactions in Neuroinflammation. In: Suzumura Akio, KI., editor. *Neuron-Glia Interaction in Neuroinflammation*. Springer; New York: 2013. p. 75-90.
55. Kinnunen A, Koenig J, Bilbe G. Repeated variable prenatal stress alters pre- and postsynaptic gene expression in the rat frontal pole. *Journal of neurochemistry*. 2003; 86(3):736–748. [PubMed: 12859686]
56. Yao I, Iida J, Nishimura W, Hata Y. Synaptic and nuclear localization of brain-enriched guanylate kinase-associated protein. *The Journal of neuroscience: the official journal of the Society for Neuroscience*. 2002; 22(13):5354–5364. [PubMed: 12097487]
57. Xu W. PSD-95-like membrane associated guanylate kinases (PSD-MAGUKs) and synaptic plasticity. *Current opinion in neurobiology*. 2011; 21(2):306–312. [PubMed: 21450454]
58. Deguchi M, Hata Y, Takeuchi M, Ide N, Hirao K, Yao I, et al. BEGAIN (brain-enriched guanylate kinase-associated protein), a novel neuronal PSD-95/SAP90-binding protein. *J Biol Chem*. 1998; 273(41):26269–26272. [PubMed: 9756850]
59. Garcia E, Mehta S, Blair L, Wells D, Shang J, Fukushima T, et al. SAP90 binds and clusters kainate receptors causing incomplete desensitization. *Neuron*. 1998; 21(4):727–739. [PubMed: 9808460]
60. Wang C-C, Chen P, Hsu C-W, Wu S-J, Lin C-T, Gean P. Valproic acid mediates the synaptic excitatory/inhibitory balance through astrocytes - A preliminary study. *Progress in neuro-psychopharmacology & biological psychiatry*. 2012; 37(1):111–120. [PubMed: 22343008]

61. Lerma J, Marques JM. Kainate receptors in health and disease. *Neuron*. 2013; 80(2):292–311. [PubMed: 24139035]
62. Tao J, Wu H, Lin Q, Wei W, Lu XH, Cattle JP, et al. Deletion of astroglial Dicer causes non-cell-autonomous neuronal dysfunction and degeneration. *J Neurosci*. 2011; 31(22):8306–8319. [PubMed: 21632951]
63. Penzes P, Cahill M, Jones K, VanLeeuwen J-E, Woolfrey K. Dendritic spine pathology in neuropsychiatric disorders. *Nature neuroscience*. 2011; 14(3):285–293. [PubMed: 21346746]
64. Jin S-G, Kadam S, Pfeifer G. Examination of the specificity of DNA methylation profiling techniques towards 5-methylcytosine and 5-hydroxymethylcytosine. *Nucleic acids research*. 2010; 38(11)

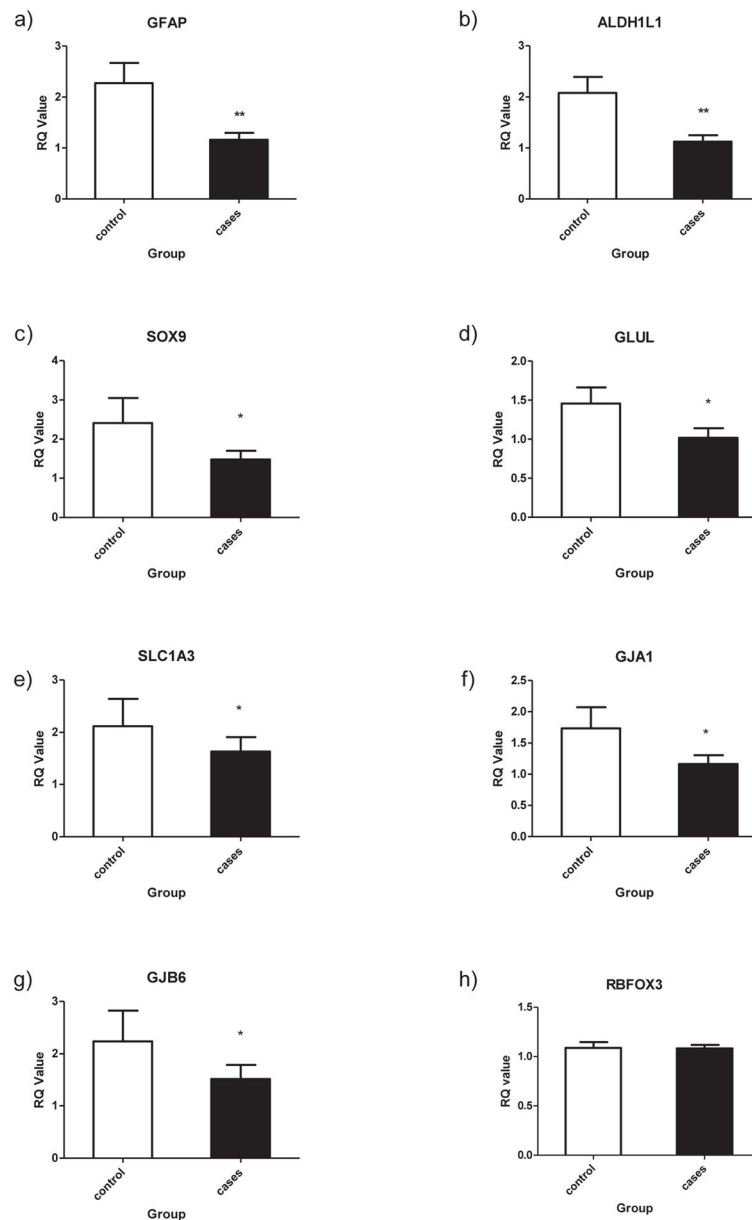
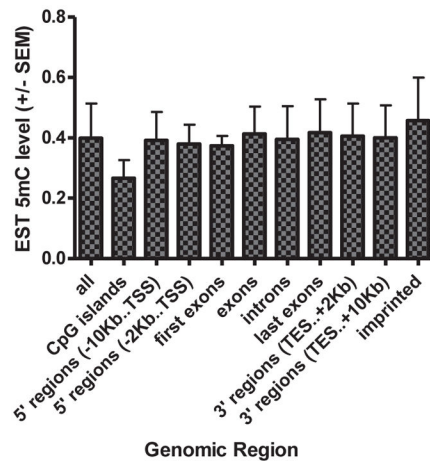


Figure 1. Screening cases and controls for astrocytic genes

Strong decrease in expression of astrocyte markers in BA 10 from cases and controls (N=121) using quantitative PCR a) GFAP (mean ± SEM), case (1.17 ± 0.13), control (2.27 ± 0.40) $p=0.0068$ and b) ALDH1L1 case (1.12 ± 0.13), control (2.08 ± 0.31), $p=0.0023$ c) SOX9 case (1.48 ± 0.22), control (2.41 ± 0.64) $p=0.03$, d) GLUL case (1.02 ± 0.12), control (1.46 ± 0.21), $p=0.01$, e) SCL1A3 case (1.63 ± 0.28), control (2.12 ± 0.52), $p=0.04$, f) GJA1 case (1.17 ± 0.14), $p=0.03$, g) GJB6 case (1.48 ± 0.23), control (2.41 ± 0.64), $p=0.05$., h) Expression of RBFOX3 (aka NeuN, a standard marker for mature neuronal identity) shows no difference between groups ($p=0.86$). (Tests performed were either Student T-test or Mann Whitney, depending on the distribution of the data)

a)



b)

Genomic region of DMR	% of DMRs (115)
first exon	0.87%
exon	2.61%
gene	33.91%
intron	31.30%
-5000bp..TSS	10.43%
TES..+5000bp	6.09%
Intergenic	56.52%

c)

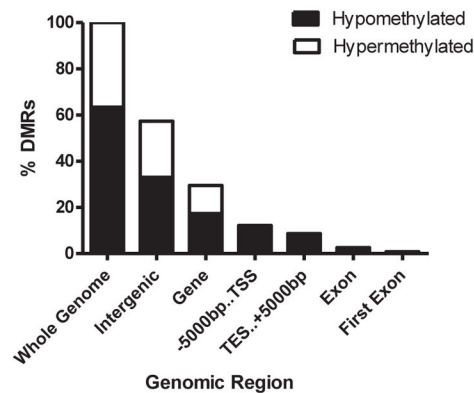


Figure 2. Estimated methylation levels across the genome and level of methylation in case relative to controls

a) Comparison of DNA methylation levels between cases and controls reveals region specific effects in the human genome. The overall methylation levels were estimated from region read counts. The Wilcoxin rank-sum test was used to determine significance of methylation differences between pairs of region types. Only introns were not different than 3' regions, all other pairs of regions types were significantly differentially methylated ($p < 2E10-22$). TSS, transcription start site; TES, transcription end site, imprinted genes are based on geneimprint.com, CpG islands are defined as regions with an expected CpG frequency of greater than 60%, a GC content of greater than 50% and a length greater than 200bp. b) the percentage summary of DMRs in known genome regions. c) cases with decreased expression of astrocyte associated genes show a genome-wide pattern of hypomethylation. 63.5% of DMRs were hypomethylated in cases compared to controls.

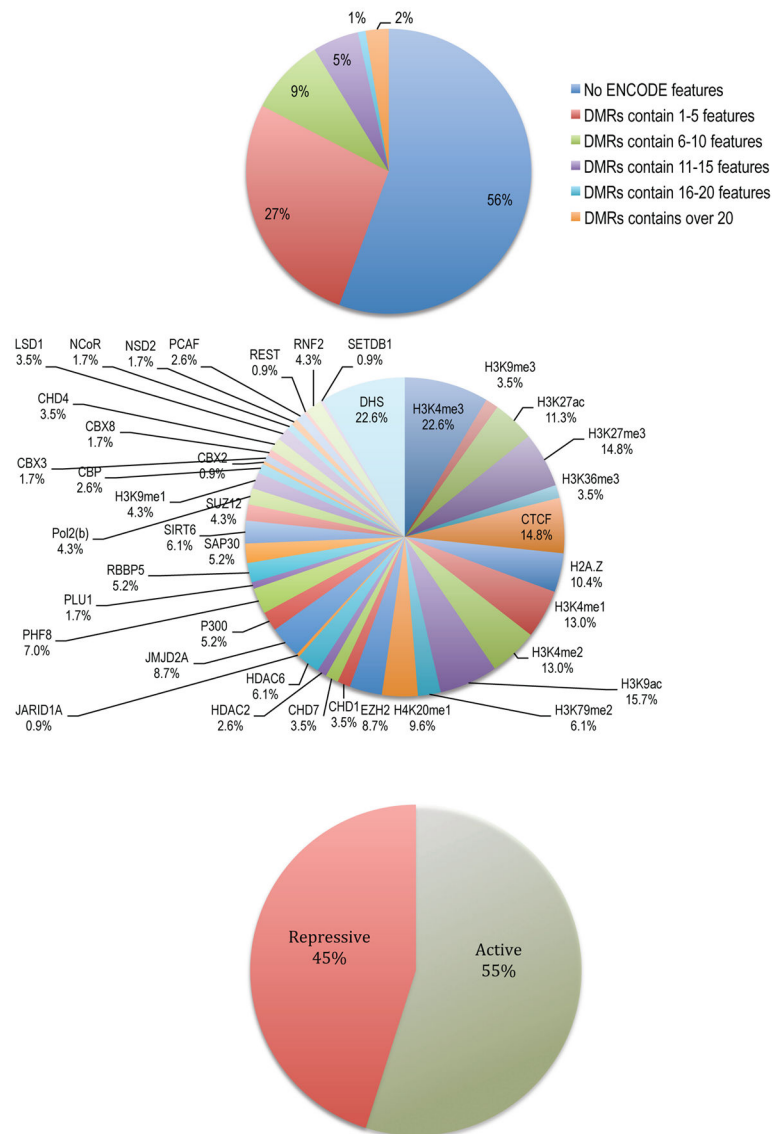


Figure 3. DMRs overlap with ENCODE data
 Strong overlap of DMRs with ENCODE data. a) 44% of DMRs overlap with at least one regulatory feature. a) the breakdown of DMRs overlapping multiple ENCODE features b) the proportion of all queried regulatory features represented within our sample. c) the breakdown of DMRs overlapping with active or repressive regulatory marks.

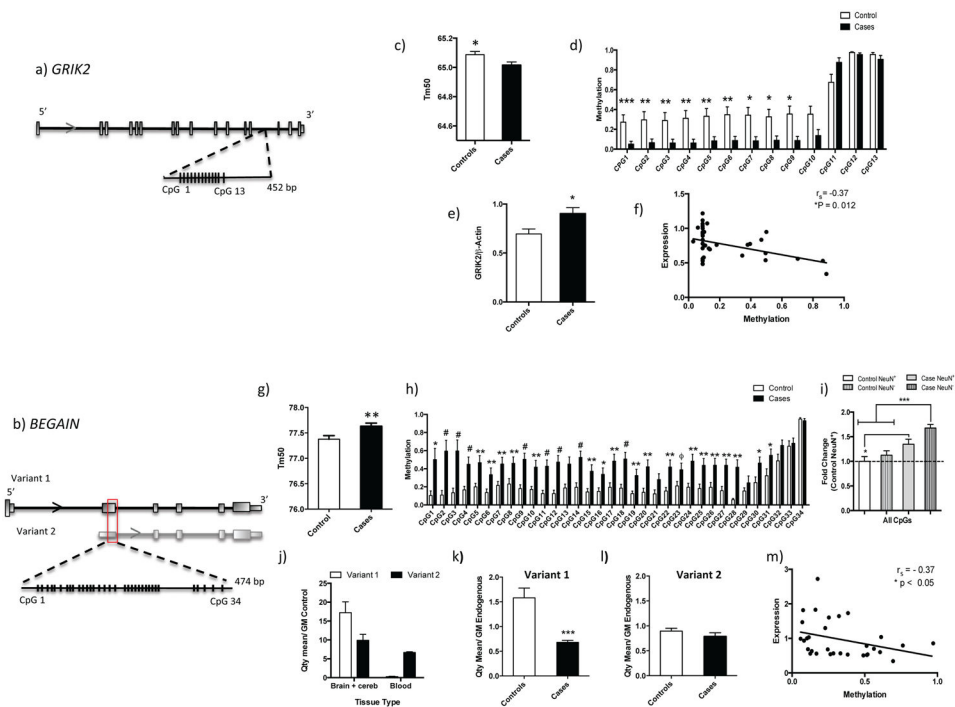


Figure 4. Gene specific validation of DMRs shows inverse correlation to gene expression levels and FAC sorting shows specific non-neuronal contribution

Schematic diagrams of each gene highlighting region of methylation difference, the size of amplicon and the number and distribution of CpGs for each a) *GRIK2* and b) *BEGAIN*, respectively. c) HRM results for *GRIK2* show a decreased methylation in cases (Unpaired t test, $p=0.025$). d) Bs-cloning supports MDB-Seq and HRM results showing a cluster of the first 9 CpGs as significantly less methylated in cases ($n=21$, avg. 17 clones/sample) than controls ($n=20$, avg. 17 clones/sample) mixed model regression analysis was performed to assess significance of methylation at each CpG, * $p<0.05$, ** $p<0.01$, *** $p<0.001$ exact values for pairwise comparison are in SI table 9a and cluster analysis in 9b). e) *GRIK2* expression as measured by relative quantitation using TAQMAN probes shows an increasing in expression in cases (student t-test $p=0.012$). f) *GRIK2* expression correlates with the cluster of significantly differentially methylated CpGs (average methylation at each CpG, spearman $r=-0.37$, $p=0.012$). g) HRM results for *BEGAIN* show more methylation in cases compared to controls with (Unpaired t test with Welch's correction, $p=0.007$). h) Bs-cloning for *BEGAIN* shows striking increase in methylation of cases ($n=17$, avg. 11 clones/sample) compared to controls ($n=18$, avg. 11 clones/sample) mixed model regression analysis was performed to assess significance of methylation at each CpG, * $p<0.05$, ** $p<0.01$, # $p<0.00$, ϕ trend 0.053, exact values for pairwise comparison are in SI table 9c and cluster analysis in 9d). Cases showed on average a three-fold increase in methylation within cluster on *BEGAIN*. i) *BEGAIN*FAC sorted samples show a strong contribution of methylation from the non-neuronal cell fraction in case samples, whereas there is no difference in controls sample methylation between the two fractions ($n=9$ for all groups, avg. 17 clones/sample, one-way Anova $F(3.32)=10.74$, $p<0.0001$, Tukey's pos-hoc, * $p<0.05$, *** $p<0.001$, *** $p<0.0001$). j) Analysis of *BEGAIN* variant expression in brain and blood. Experiment

was independently repeated 3 times with 2 endogenous controls per experiment, geometric mean of endogenous control was calculated and expression was normalized to this value. We qualitatively show that variant 1 is more expressed in brain and almost not present in blood, while we still detect variant 2 in blood. k) The astrocytic dysfunction group show a 2.3 fold decrease in the expression of *BEGAIN* Variant-1 compared to controls (Mann Whitney test $p < 0.0001$), l) whereas variant-2 shows no change (Student t-test, $p = 0.26$) m) The decrease in variant-1 expression correlates with the significantly differentially methylated cluster of CpGs in *BEGAIN* (average methylation at each CpG, spearman $r = -0.37$, $p = 0.019$).

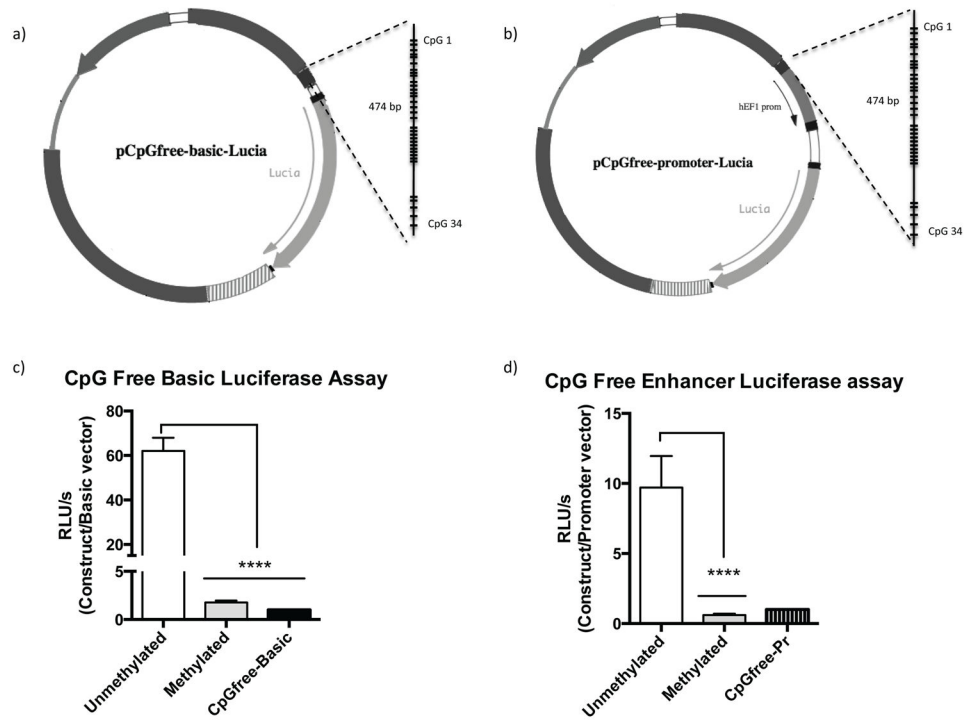


Figure 5. Promoter and enhancer properties repressed by DNA methylation in BEGAIN 474bp amplicon

Schematic diagram of CpG free lucia reporter vector with a) no endogeneous promoter and b) behind the human EF-1 α promoter and placement of 474bp insert into multiple cloning site c) The unmethylated insert shows promoter activity which is completely abolished by methylation (10 replicates/group, One-way Anova F (2,27)=106.8, $p<0.0001$, Tukey's post-hoc **** $p<0.0001$). d) Placed in front of the promoter, the 474 bp insert showed enhancer activity again showing complete repression of activity by methylation (10 replicates/group, One-way Anova F (2,23)=17.80, $p<0.0001$, Holm-Sidak's post-hoc, *** $p<0.001$ **** $p<0.0001$).

Table 1

The list of astrocyte associated genes within the dataset

These genes were selected based on functions such as cation homeostasis, response to oxidative stress, and glutamatergic synaptic transmission. Genes were supplemented by the addition of genes described by Cahoy et al.³⁰ as enriched in astrocytes. Some genes have multiple windows of methylation differences; altogether this list represents 7 DMRs of the previously described 34 gene based DMRs (~21%). *Meth status* refers to whether the regions show an increase (↑) or decrease (↓) in methylation. *ENCODE overlap* refers to either DHS or H3K4me3, both or no overlap with the DMR. *Region* describes the general genomic region where the DMR is found for that gene. *Strand* refers to the location of the genes, either on the sense (+) or antisense (-) strand. *Avg log₂ fold change* is the absolute difference of methylation at that site, it is averaged to account for the multiple windows (DMRs) found in the gene. *Avg Adj p value* is the significance of the fold change adjusted to correct for multiple testing, averaged as before. *# of win* is the number of windows found within that gene; a window represents a differentially methylated region. *Function* is a brief functional description of the gene. The list is ranked by DMR containing windows, and then lowest avg adj p value and avg log₂ fold change.

Chr	Gene Name	Meth Status	ENCODE Overlap	Regions	Strand	Avg Log ₂ Fold change	Avg Adj P value	# of Win	Function
6	<i>GRIK2</i>	↓	None	intronic	+	1.44	0.09	2	Glutamate ionotropic kainate receptor
10	<i>NEBL</i>	↓	None	intronic	-	2.00	0.11	2	Actin-binding related protein
3	<i>PVRL3</i>	↑	None	intronic	+	2.96	0.08	1	Adhesion molecule at adhesion junctions
*3	<i>ROPN1B</i>	↑	Both	downstream of TES	-	1.04	0.01	2	signal transduction

* This DMR is technically not in the primary variant of *ROPN1B*.